1 **The pyriproxyfen metabolite 4'OH- pyriproxyfen disrupts thyroid hormone signaling and**
2 **enhances Musashi-1 levels in neuroprogenitors.**

3 Petra Spirhanzlova[1]; Sébastien Le Mével[1]; Karn Wejaphikul[2] ; Bilal Mughal[1]; Jean-David
4 Gothié[1]; Anthony Sébillot[1]; Lucille Butruille; Michelle Leemans[1] ,Theo Visser+[2] ; Sylvie
5 Remaud[1]; Jean-Baptiste Fini[1] and Barbara Demeneix[1]

6 [1]UMR CNRS 7221, Evolution des Régulations Endocriniennes, Muséum National d'Histoire
7 Naturelle, Sorbonne Université, 75231 Paris, France.
8 [2]Department of Internal Medicine and Rotterdam Thyroid Center, Erasmus University Medical
9 Center, Rotterdam, The Netherlands.
10
11 Correspondence and requests for materials should be addressed to B.A.D.
12 (email:bdem@mnhn.fr)

13 Epidemiological and experimental studies have raised questions as to whether the insecticide
14 pyriproxyfen (PPF) could be implicated in the increased incidence of microcephaly associated
15 with ZIKA infection during pregnancy. This pesticide is documented as a thyroid hormone (TH)
16 disrupting chemical. We investigated whether environmentally relevant amounts of its main
17 metabolite, 4'-OH-pyriproxyfen (4'-OH-PPF), modified TH signaling and early neuronal
18 development. First, an *in silico* study revealed strong affinity of 4'-OH-PPF to fit the ligand
19 binding pocket of TH receptors (TRs). Further, *in vitro* assays on human cell lines showed 4'OH-
20 PPF (> 3 mg/L ) to act as a TRα antagonist. Next, using a transgenic Xenopus TH-sensitive
21 reporter system, Tg(*thibz*:GFP) tadpoles showed that 4'OH-PPF (> $10^{-7}$ mg/L) displayed TH-
22 disruptive activity and reduced tadpole mobility (> $10^{-1}$ mg/L). Exposure to 4'OH-PPF
23 significantly reduced Xenopus head size at levels equivalent to the maximum recommended daily
24 intake of PPF (3x $10^{-1}$ mg/L). Most strikingly, in both the Xenopus system *in vivo* and in mouse
25 neurosphere cultures, environmentally relevant concentrations of 4'OH-PPF increased expression
26 of the gene encoding an RNA-binding protein that enables ZIKA replication: Musashi-1 *(msi1)* in
27 neurogenic brain areas. We conclude that first, the PPF metabolite, 4'OH-PPF, disrupts thyroid
28 signaling, neuronal development and behavior in Xenopus embryos, and second, that it increases
29 Musashi-1 levels in neurogenic zones of both mouse and Xenopus, creating the potential to
30 enhance viral replication. As PPF is used in areas with high microcephaly incidence and is
31 readily broken down to 4'OH-PPF, these findings provide a plausible mechanism whereby PPF
32 could, through modulating expression of Musashi-1, exacerbate the effects of ZIKA virus
33 infection.

34 Key words: pyriproxyfen, thyroid hormone, musashi 1, brain development

**Introduction**

A number of lines of evidence link infection by the ZIKA virus to the increased incidence of microcephaly in Central and South America starting from early 2016 (Alvarado and Schwartz, 2017; de Araújo et al., 2016; Faizan et al., 2016; de Oliveira et al., 2017). However, many authors have queried as to whether other environmental factors could contribute to the increased incidence of microcephaly (Butler, 2016a, 2016b; Rodrigues and Paixao, 2017). Certain authors have queried whether the use of the pesticide pyriproxyfen (PPF) could be implicated (de Albuquerque et al., 2016; Evans et al., 2016; Parens et al., 2017; REDUAS, 2016). PPF was first introduced into Brazilian drinking water in late 2014 as a mean of controlling the *Aedes aegypti* mosquito population, the vector for the ZIKA virus. Highest amounts of PPF were used in the north-east, but whether or not the pesticide had any toxic effects, related or not to microcephaly was not thoroughly investigated, neither epidemiologically nor experimentally until recently (Parens et al., 2017).

PPF is a juvenile hormone analog primarily used against household insects including fleas and on agricultural crops and its use has been approved worldwide (US EPA, 2011; WHO, 2007; Wilson, 2004). WHO recommends that daily intake of PPF should not exceed 0.3 mg/L for an average adult and the recommended concentration of PPF in drinking water containers is 0.01 mg/L (WHO, 2007). The use of PPF is not limited only to South America. PPF has been added in the drinking water in Cambodia or Malaysia and it has been found in Spanish river water and fish at concentrations reaching 90 ng/L and 0.1-0.3 ng/g respectively (Belenguer et al., 2014; Invest and Lucas, 2008). However, PPF has been documented as interfering with thyroid hormone (TH) signaling (Wegner et al., 2016) an essential hormone for brain development (Bernal, 2005).

The major pathway of PPF metabolism is hydroxylation at the 4'-position, producing majoritarily 4'-OH-PPF in Xenopus, mice, rats, goats, house flies and chicken (Fujimori, 1999; Ose et al., 2017; Yoshino et al., 1995; Zhang et al., 1998). To our knowledge, no studies have yet assessed the toxicological potential of 4'-OH- PPF.

Given the lack of information on 4'-OH-PPF, we used *Xenopus laevis* tadpoles, a well-known model for testing TH disruption (Fini et al., 2012, 2017) and mouse neurospheres to investigate the potential of PPF and 4'-OH-PPF to disrupt thyroid hormone (TH), signaling during brain development. We also examined how PPF and 4'-OH-PPF affected expression of the key protein, Musashi-1 known to be required for ZIKA replication (Chavali et al., 2017). *Musashi-1* is down

66  regulated by TH in the neurogenic zone of the adult mouse brain (López-Juárez et al., 2012), one
67  example of the multiple processes implicating TH during the development of the central and
68  peripheral nervous system, from stem cell proliferation, lineage decisions, differentiation,
69  migration, synaptogenesis and myelination (Bernal, 2005; Morreale de Escobar et al., 2004).
70  Impaired thyroid signaling during  development results in brain defects in human (Korevaar et
71  al., 2016; Pop et al., 1999).

72

## Materials and methods

### 1. Materials

*1.1 Reagents*

76  3,3′,5-Triiodo-L-thyronine sodium salt (T$_3$) (Sigma -  CAS 55-06-1), 4'OH pyriproxyfen (HPC –
77  Ref. 675366), Pyriproxyfen (Sigma – CAS 95737-68-1), Dimethyl sulfoxide –DMSO (Sigma -
78  CAS 67-68-5), DMEM/F12 (Gibco), Ethyl 3-aminobenzoate methanesulfonate salt (MS 222)
79  (Sigma - CAS 886-86-2), NH3 (synthetized by AGV Discovery-France), Sodium bicarbonate
80  (Sigma- CAS 144-55-8), Paraformaldehyde (Sigma – CAS 30525-89-4), Succrose (Sigma- CAS
81  57-50-1), Ethylen glycol (Sigma- CAS 107-21-1), Tris, pH 8.0, KCl, MgCl$_2$, glycerol, DTT
82  (Sigma), [$^{125}$I]T$_3$,  Agilent RNA 6000 Pico Kit,  Reverse Transcription Master Mix (Fluidigm),
83  Power SYBR Master Mix (Life technologies - ref.4368708), RNAqueous –micro kit (Life
84  technologies - ref. AM1931), Primers (Eurofins), TNT® T7 Quick Coupled
85  Transcription/Translation System (Promega, Leiden, The Netherlands), nitrocellulose membrane
86  (Millipore HA filters, 0.45 μm), BSA, Normal goat serum, Papain, Cysteine and DNAse, FGF2
87  (Peprotech), TaqMan Preamp MasterMix, TaqMan Universal PCR MasterMix (both
88  ThermoFisher), specific TaqMan probes (*Msi1*, Mm00485224_m1; *ActB*, Mm01205647_g1;
89  *Gapdh*, Mm99999915_g1; *Hprt*, Mm00446968_m1), Msi1 primary antibody (Rabbit polyclonal
90  to Msi1- Abcam, UK), Alexa Fluor 488-conjugated anti-rabbit antibody (Thermofisher
91  Scientific),  Milli-Q reference water, Nuclease free water, Evian water in glass bottle 75 cL or
92  another mineral water with reproducible quality, Liquid nitrogen.

93

94

95    *1.2 Equipment*

96    Electrical devices: BioAnalyzer (Agilent), Daniovision (Noldus), Fluorescent microscope

97    equipped with 25x objective and long pass GFP filter – Olympus, Incubator, NanoDrop

98    ThermoScientific, QuantStudio 6 flex QPCR machine (Life technologies), PCR machine

99    (Biorad), Vortex mixer.

100   Laboratory utensils: 384-well hardshell plate clear, 50 mL Greiner capped tubes (Greiner Bio-one

101   - ref.227261), 96-well black, conic well plate (Greiner Bio-one - ref. 651209) , Adhesive  covers

102   for 384 well plates, Sterile dissecting tools, Microcentrifuge tubes 0.2 -1.7 mL, flip top, Multi-

103   distribution pipette , PCR tube Strips 0.2 mL Eppendorf, Micropipettes, Pipette tips 0.2-5000 µL,

104   Transfer pipets with extended fine tip, Transparent flat 6-well plates (TPP, Switzerland),

105   Transparent flat 12-well plates (TPP, Switzerland).

106   *1.3  Software:*

107   Capture pro (QImaging), ImageJ – optional, GraphPad Prism 7, MS Excel, QuantStudio™ Real-

108   Time PCR Software, Ethovision XT 11.5, Qiagen CLC Drug discovery 3, NHR scan.

109   **2.  Methods**

110   *2.1 In silico*

111   Qiagen CLC Drug discovery 3 was used to assess ligand-protein interactions. Human crystal

112   structure of thyroid hormone receptor alpha (TRα, 4LNW), bound to a ligand was used. The list

113   of compounds including pesticides and insecticides used have been outlined in supplementary

114   table 1 with their corresponding PubChem compound id. Thyroid hormone antagonist NH3 (Lim

115   et al., 2002) and 4'-OH-PPF were drawn manually. 10,000 iterations were run for each ligand-

116   protein interaction, against the $T_3$ binding pocket of TRα, and top 10 recurring interactions were

117   analysed. The "score" represents the steric fit of ligand in the $T_3$ binding pocket, where a more

118   negative score indicates a higher ligand-protein interaction. Mean of top 10 interactions scored

119   were ranked and displayed in supplementary table 1.

120

121

122

4

123 *2.2 Cell culture, transfection, and luciferase assays*

124 JEG3-cell culture and transfection were performed as previously described (van Gucht et al.,
125 2016). Briefly, FLAG-tagged human TRα1 was overexpressed in JEG3 cells together with a
126 DR4-TRE luciferase reporter construct and pMaxGFP as a transfection control. After 24 hours,
127 cells were incubated for 24 hours in DMEM/F12+0.1% BSA containing 1 nM of T3 and the
128 indicated concentrations of 4'-OH-PPF or the TRα1-antagonist, NH3. Luciferase activity was
129 measured in cell lysates as previously described (van Mullem et al., 2012). The ratio of the
130 luciferase and GFP activities was calculated to correct for transfection efficiency. The results are
131 expressed as percentage of the ratio at 0 nM 4'-OH-PPF or NH3. Data from two independent
132 experiments performed in triplicate are shown as mean±SEM and analysed by One-way ANOVA
133 with Tukey's post-test. Statistical significance was considered when p-values < 0.05.

134 *2.3 [$^{125}$I]T3 competitive binding assays*

135 FLAG-tagged TRα1 protein was synthesized by the TNT® T7 Quick Coupled
136 Transcription/Translation System (Promega, Leiden, The Netherlands), according to the
137 manufacturers' protocol. 0.25 μL of TRα1 protein was incubated for 2 hours at 30°C in binding
138 buffer (20 mM Tris, pH 8.0, 50 mM KCl, 1 mM MgCl$_2$, 10% glycerol, 5 mM DTT) containing
139 0.02 nM of [$^{125}$I]T$_3$ and 0-10,000 nM of the unlabelled competitive compound (T$_3$, 4'-OH-PPF,
140 or NH3). Subsequently, samples were filtered through a nitrocellulose membrane (Millipore HA
141 filters, 0.45 μm). The amount of TR-bound [$^{125}$I]T$_3$ on the membranes was quantified and
142 expressed as percentage maximal [$^{125}$I]T$_3$ binding for each competitor. The [$^{125}$I]T$_3$ dissociation
143 curve and the dissociation constant (Kd) were computed using GraphPad Prism version 7.0
144 (GraphPad, La Jolla, CA). The data were shown as mean±SEM of at least two independent
145 experiments performed in duplicate.

146 *2.4 Primary mouse NSC neurosphere cultures*

147 C57BL/6 wild-type male mice, eight weeks old, were purchased from Janvier (Le Genest St. Isle,
148 France). Food and water were available ad libitum. All procedures were conducted according to
149 the principles and procedures in Guidelines for Care and Use of Laboratory Animals, and
150 validated by local and national ethical committees. Five mice were sacrificed per neurosphere
151 culture. Brains were removed and lateral SVZ dissected under a binocular dissection microscope
152 in DMEM-F12-glutamax 1/50 Glc 45% and incubated with papain, cysteine and DNAse for 30

153  min at 37°C with pipette dissociation every 10 min to obtain a single-cell suspension. Cells were

154  collected by centrifugation (1000 rcf, 5 min). After resuspension, cells were equally distributed in

155  wells of 96-well plates and cultured in complete culture medium (DMEM-F12 [Gibco], 40

156  µg/mL insulin [Sigma], 1/200 B-27 supplement [Gibco], 1/100 N-2 supplement [Gibco], 0.3%

157  glucose, 5 mM Hepes, 100 U/ml penicillin/streptomycin) containing 20 ng/mL of EGF and 20

158  ng/mL of FGF2 (Peprotech), in a 5% $CO_2$ environment at 37°C for seven days to obtain primary

159  neurospheres. To test the effect of $T_3$ and 4'OH-PPF on neurosphere formation, $T_3$ (10nM) and/or

160  4'OH-PPF ($10^{-2}$mg/L, $10^{-1}$ mg/L or $3x10^{-1}$ mg/L) was added to the proliferation medium (12 wells

161  per condition). Medium was renewed every two days.

162

### 2.5 Gene expression analysis – mouse neurospheres

164  After seven days proliferation, neurospheres grown in the same condition were pooled, and RNA

165  was extracted (ThermoFisher RNAqueous MicroKit) and retro-transcriptions performed

166  (Fluidigm) following manufacturers' instructions. Preamplifications (10 cycles) and qPCR were

167  performed using TaqMan Preamp MasterMix and TaqMan Universal PCR MasterMix,

168  respectively (ThermoFisher), and specific TaqMan probes (References: *Msi1*, Mm00485224_m1;

169  *ActB*, Mm01205647_g1; *Gapdh*, Mm99999915_g1; *Hprt*, Mm00446968_m1) following

170  manufacturer's instructions. Every qPCR amplification was run in triplicate. ΔCt have been

171  calculated between target genes and the geometrical mean of three endogenous controls, *ActB*,

172  *Gapdh* and *Hprt*, for each sample. Differences between control and treated groups (ΔΔCt) were

173  used to calculate fold-increases ($2^{-\Delta\Delta CT}$) and to determine changes in target genes expression.

174

### 2.6 Chemical exposure - Xenopus laevis tadpoles

176  The stock solutions of PPF and 4'-OH- PPF were prepared according to following protocol: 15

177  mg of PPF or 4'-OH- PPF were dissolved in 5 ml of DMSO to create a 3g/L stock solution

178  (stored at -20°C). Final exposure solution was prepared every day of exposure using fresh

179  aliquots of stock solutions (prepared by cascade dilutions from 3g/L stock) by adding 1µL of

180  stock solution to 10 mL of Evian water. All groups including control contained 0.01% DMSO.

181  Fifteen NF 45 TH/bZip eGFP *Xenopus laevis* tadpoles were placed into each well of 6-well plate.

182  Each well corresponds to one exposure group. Eight mL of previously prepared final exposure

183   solution was added into the corresponding well. Tadpoles were exposed for 72 hours at 23°C in

184   dark with daily renewal at the same hour for the XETA assay. For brain gene analysis exposure

185   was limited to 24 hours. Tadpoles were exposed to both PPF and 4'-OH-PPF in the presence and

186   the absence of 5nM $T_3$, the most biologically active form of TH.

*2.7  XETA - Imaging*

188   At the end of the exposure, tadpoles were rinsed in Evian and anaesthetized using MS-222 (100

189   mg/L; Stock 1g/L- 1g of MS-222 and 1g of sodium bicarbonate dissolved in 1 L of animal water,

190   pH adjusted to pH 7.4-8; stock diluted 10x in animal water). One anaesthetized Tg(*thibz*:GFP)

191   tadpole was placed per well into 96-well plate (black, conic based) and positioned using a fine

192   transfer pipette so the ventral region of the tadpole was facing upwards. To acquire color images

193   we used Olympus AX-70 binocular equipped with 25x objective, long pass GFP filters and a Q-

194   Imaging Exi Aqa video camera. Images were captured using the program QC Capture pro

195   (QImaging) with 3s exposure time. After the image acquisition, tadpoles were euthanized in MS-

196   222 1g/L, fixed overnight in paraformaldehyde 4% and stored at -20°C in cryoprotectant (150g of

197   sucrose and 150 mL of ethylen glycol qsp to 500 mL by PBS 1x). Using the program ImageJ

198   non-specific signal was excluded by splitting the image into 3 layers (red, blue and green

199   channel) followed by subtraction of the red and blue channel from the green one. Integrated

200   density of the green channel was then quantified. Statistical analysis was performed in the

201   program GraphPad Prism 7. Tests used to each experiment are described in the figure legends.

*2.8 RT-qPCR – Xenopus laevis tadpole brains*

203   At the end of the 24h exposure, tadpoles were rinsed and anaesthetized in 100 mg/L MS-222.

204   RNA-free dissecting tools were used to dissect tadpole brains. Two brains were placed in one

205   microdissection tube (nuclease free) containing 100 µL lysis solutions from an RNA extraction

206   kit (Ambion RNAqueous). Liquid nitrogen was used to snap freeze the tubes which were then

207   stored at -80°C prior to RNA extraction according to the manufacturer's instructions. The RIN of

208   each sample was verified using Agilent biaonalyzer. Only samples with RIN higher than 7.5 were

209   used for further RT-qPCR. cDNA was synthetized using Reverse Transcription Master Mix

210   (Fluidigm). The synthetized cDNA was 20x diluted (5µL of DNA in 95µL of nuclease free

211   water). qPCR mix contained following components: 0.15 µL of reverse primer (10pM), 0.15 µL

212   of forward primer (10pM), 1.7 µL of nuclease free water and 3 µL of Power SYBR master mix

213    per reaction. For the final reaction 5 µL of previously prepared qPCR mix were added in one well

214    of 382 well-plate together with 1µL of diluted cDNA. Water control and RT- control was

215    included on every plate. Comparative $C_t$ measurements including melt curve were quantified

216    using QuantStudio 6 flex qPCR device (Life technologies). $C_t$ value of each sample was exported

217    in excel format. Geometric mean of two housekeeping genes (*ef1a* and *odc*) of each sample was

218    quantified and excluded from the Ct values corresponding to the sample (resulting in $\Delta C_t$ value).

219    Median values of control group of each gene was calculated and extracted from each $\Delta C_t$ value to

220    normalize. Fold change using formula =(power 2; - $\Delta C_t$ value of a sample) was calculated and

221    statistical analysis using resulting values was performed using the program Graphpad Prism7.

222

223    *2.9 Immunohistochemistry in Xenopus laevis tadpole brains*

224    After 24h of exposure, tadpoles were euthanized using MS-222 (1g/L) and fixed in 4%

225    paraformaldehyde for 3h at room temperature. After the fixing period the brains of the tadpoles

226    were dissected and placed in PBT (1% Triton X-100 in PBS) for at least 18h at 4°C. Next the

227    brains were blocked in 10% (vol/vol) normal goat serum (NGS) in PBT for 3h at 4°C. The

228    primary antibody (Rabbit polyclonal to Msi1- Abcam, UK) was diluted 1/300 in 10% NGS in

229    PBT and the brains were incubated in the solution over night at 4°C. Next morning, the plates

230    were removed to RT for 1h prior to multiple washes in PBT during a period of at least 8 hours.

231    Secondary antibody (Alexa Fluor 488-conjugated anti-rabbit (Thermofisher Scientific) diluted

232    1/400 in 10% NGS in PBT was applied over night at 4°C. After the secondary antibody

233    treatment, brains were washed several times in PBS during the period of 4 hours. Images of the

234    dorsal side of the brains were taken using Leica MZ16F stereomicroscope equipped by QImaging

235    Retiga-SRV camera. Images were analyzed using the program ImageJ. Region of interest was

236    manually selected and the mean integrated density of each image was calculated with the

237    threshold set to 60.

238    *2.10    Mobility of Xenopus laevis tadpoles*

239    After 72h exposure tadpoles were rinsed in Evian water and placed in 12-well plates with one

240    tadpole per well each containing 4 mL Evian water. Each group was given 10 minutes

241    acclimatization time prior to the trial. Tadpole movements were traced for 10 minutes with 30s

242    light/30s dark intervals using a Daniovision (Noldus) device. Total distance traveled during each

243    10s of the 10min trials were quantified and exported using the Ethiovision XT 1.5 program. All

244    values were normalized to the mean of the control group of the 0s-10s time period.

245

246    *2.11    Structural measurements of Xenopus laevis tadpole brains*

247    Tadpoles previously fixed in step 2.7 were placed in a Petri dish and manually positioned to

248    expose the dorsal part of the body. Color images of tadpole heads on black background were

249    taken using a Leica MZ16F stereomicroscope equipped by QImaging Retiga-SRV camera. Brain

250    structures were measured in program ImageJ. MS Excel was used to calculate head/brain ratio.

251

252    *2.12    Statistical analysis*

253    Statistical analysis was performed using program Graph Pad Prism 7. The D'Agostino & Pearson

254    normality test was done to determine if values follow Gaussian distribution (parametric) or not

255    (non-parametric). One way ANOVA was done in the case of parametric distribution and followed

256    by Dunnett's multiple comparison post-test. For results displaying non-parametric distribution,

257    Kruskal-Wallis test with Dunn's multiple comparison post-test was used. If only two groups were

258    compared, t-test (parametric) or Mann-Whitney's test (non-parametric) was used.

259

260

## 3. Results

### 3.1.    *Comparative binding scores predict a strong steric fit into the T3 binding pocket*

A comparative ligand-protein interaction of common insecticides, TH and TH analogues against the human thyroid hormone receptors TRα was carried out and ranked according to their degree of interaction (Supplementary table 1). $T_3$, 4'-OH-PPF and PPF ligands show comparative binding scores -62.83 and -76.47 (Fig 1A) and -73.3 (Fig S1) respectively for TRα. These scores predict a strong steric fit of 4'-OH-PPF and PPF, in a similar fashion to $T_3$, into the $T_3$ binding pocket. With the same method, NH3 displayed comparative binding scores of -78.7 for TRα.

### 3.2.    *High concentrations of 4'OH-PPF inhibit $T_3$-induced transcriptional activity of TRα1*

The effect of 4'-OH-PPF on the $T_3$-induced transcriptional activity of TRα1 was determined by an *in vitro* luciferase reporter assay using human placenta JEG3-cell cultures. Transcriptional activity was significantly decreased by the highest concentration of 4'-OH-PPF (3 mg/L) (Fig.1B). NH3 also reduced the transcriptional activity of TRα1, but already at lower concentrations (4.7 and 4.7x $10^{-1}$ mg/L) (Fig.1C). These findings shown 4'-OH-PPF can interfere with $T_3$-induced transcriptional activity of TRα1, but only at a high dose, consistent with the low affinity binding to the receptor.

### 3.3.    *4'-OH-PPF binds to TRα1 with low affinity*

[$^{125}$I]T3 competitive binding assays were performed to determine whether 4'-OH-PPF binds to the TRα1 receptor. Unlabelled $T_3$ and NH3, were included as positive controls. The Kd of the NH3 was 60-fold higher than the $K_d$ of unlabelled $T_3$ (21.6 vs. 0.32 nM), suggesting that NH3 can bind to the TRα1 receptor with a lower affinity than $T_3$. Competitive binding of 4'-OH-PPF to TRα1 only occurred at the highest concentration (3 mg/L) and the estimated $K_d$ of 4'-OH-PPF (~1.2 μM) was more than 3000-fold higher than $T_3$ and 50-fold higher than NH3 (Fig 1D).

10

289 *3.4.    PPF and 4'-OH- PPF affect TH signaling in the XETA assay*

290 Transgenic Tg(*thibz*:GFP) tadpoles were exposed to environmentally-relevant dose ranges of 4'-

291 OH-PPF or PPF in the presence or absence of $T_3$ (5nM). The concentrations selected varied from

292 0.1 ng/L through 100ng/l (concentration of PPF detected in the surface water in Spain (Belenguer

293 et al., 2014), 0.01mg/L – PPF drinking water limit according to WHO, up to the WHO acceptable

294 PPF daily intake level ($3 \times 10^{-1}$ mg/L) (WHO, 2007).

295 PPF, in the absence of $T_3$, significantly reduced GFP fluorescence emitted from the tadpole head

296 region at the following concentrations: $10^{-5}$, $10^{-4}$, $10^{-2}$ and $3 \times 10^{-1}$ mg/L (Fig. S2A). In the

297 presence of $T_3$, PPF did not exhibit any thyroid hormone disrupting activity (Fig S2B). In

298 contrast, 4'-OH- PPF was not active without $T_3$ (Fig 2B), but in its presence, all concentrations of

299 4'-OH- PPF significantly reduced the GFP signal (Fig 2C). These results suggest that both PPF

300 and its metabolite 4'-OH- PPF exhibit TH- disrupting properties, but that the parent compound is

301 active in the absence of $T_3$ whereas the metabolite antagonizes the effects of $T_3$.

302 *3.5.    PPF and 4'-OH- PPF affect tadpole mobility*

303 Tadpoles exposed to PPF for  72 h reacted to the light stimulus but moved significantly less than

304 controls (Fig S2C-H). Significant differences were observed in tadpoles exposed to all

305 concentrations of PPF with the exception of $10^{-3}$ mg/L. In the case of 4'-OH-PPF, the tadpoles

306 exhibited reduced mobility compared to controls, reaching significance at the two highest

307 concentrations ($10^{-1}$ and $3 \times 10^{-1}$ mg/L)(Fig 2D,E).

308 *3.6.    PPF and 4'-OH- PPF affect brain morphology*

309 The total head and brain area was measured using the ImageJ program.  Head /brain ratio was

310 calculated using MS Excel. PPF did not affect brain or head size, nor was the head/brain size

311 ratio significantly different compared to controls (Fig S4C-E). However, tadpoles exposed to

312 $3 \times 10^{-1}$ mg/L of 4'-OH-PPF exhibited significantly smaller heads compared to control (Fig 2F),

313 thus resulting in biased brain/head ratios (Fig 2H), however the brain size of these tadpoles was

314 not affected (Fig 2G). The width and length of brain compartements were meassured (Fig S4B).

315 The width of forebrain (H1) was increased in tadpoles exposed to PPF at concentrations $10^{-4}$

316 mg/L – $10^{-1}$ mg/L (Fig S4F). The width of midbrain (H3) was significantly increased in tadpoles

317 exposed to concentrations of PPF $10^{-3}$ mg/L and higher (Fig S4H). The length of the whole brain

11

318    (L3) was significantly increased by exposure to PPF at concentration $10^{-3}$ mg/L and higher (Fig

319    Fig S4H). In the case of 4'-OH- PPF, the lowest concentration $10^{-5}$ mg/L significantly increased

320    the width of forebrain and midbrain junction (Fig S4M) and the width of midbrain (Fig S4N).

321    *3.7.    PPF and 4'-OH- PPF affect brain musashi-1 gene and protein expression in Xenopus*

322    *laevis tadpoles*

323    We studied the consequences of a 24h exposure with PPF or 4'-OH PPF on brain gene *musashi-1*

324    (*msi1*) expression and its encoded protein in Xenopus *in vivo*. *Msi1* brain gene and protein

325    expression was analyzed following 24h exposure to each compound as a function of results seen

326    in the XETA test. Thus, PPF was run without $T_3$ whereas 4'-OH-PPF was tested in the presence

327    5nM $T_3$.  $T_3$ 5nM significantly reduced the expression of *msi1* gene and its encoded protein (Fig 3

328    A-C). 4'-OH-PPF increased the expression of *msi1* gene at both concentrations tested in the

329    presence of $T_3$ 5nM (Fig 3B) and increased msi1 protein expression at $10^{-2}$ mg/L (Fig 3C). PPF

330    did not affect *msi1* gene expression (Fig S3A) however the highest concentration $3x10^{-1}$ mg/L

331    significantly reduced the expression of msi1 protein in the brain of NF45 tadpoles after 24 hours

332    (Fig S3B).

333    3.8.    *4'-OH- PPF increases Msi1 gene expression in mouse neurospheres*

334    *Msi1* gene expression in mouse neurospheres after 7 d proliferation in the presence of 4'-OH-PPF

335    was analyzed by RT-qPCR. The expression of *Msi1* gene was increased 3-fold by $T_3$ 10 nM and

336    the highest concentration of 4'-OH-PPF $3x10^{-1}$ mg/L in the presence and absence of $T_3$ 10 nM

337    (fold induction 10 and 14 respectively) (Fig 3D).

338

## 4. Discussion

Given paucity and the contradictory nature of studies on the potentially adverse effects of PPF, we investigated whether its main metabolite, 4'-OH-PPF, affects TH signaling and *Msi1* gene expression using *in silico*, *in vitro* and *in vivo* approaches. TH modulates every stage of brain development, thus any modification of TH availability and action could have direct consequences on neurogenesis and brain morphology, as well as on cranio-facial development (Bernal, 2005). The importance of TH for brain development, and notably for regulating *Musashi 1* gene expression in neuroprogenitor cells (López-Juárez et al., 2012), raised the question as to whether TH disruption caused by PPF exposure might be implicated in the severity of the incidence of microcephaly in certain regions of Brazil, especially North Eastern Brazil (area with the highest incidence of microcephaly), where it has been used intensively (Parens et al., 2017).

The *in silico* results revealed that 4'-OH- PPF had a high steric fit for both TRα we tested whether the metabolite blocked $T_3$ binding to the TR LBDs. The *in vitro* study showed that 4'-OH-PPF acts as TRα antagonist at a concentration 3 mg/L, approximately 10x the WHO recommended daily intake of PPF (WHO, 2007) (Fig. 1B,D). These findings indicate that although TRα1 can bind 4'-OH-PPF , the affinity is much lower than for $T_3$ and NH3, which is not in accordance with predicted strong steric fit of 4'-OH-PPF into the $T_3$ binding pocket as shown by *in silico* docking.

However, our findings that 4'-OH-PPF affects expression *msi1* gene and protein offer a plausible mechanism to explain potential increase of susceptibility to ZIKV. We show that 4'-OH-PPF increased the levels of *msi1* gene and its encoded protein in the brain area of early stage tadpoles in the presence of $T_3$ 5nM and increased the expression of *Msi1* gene in adult mouse neurospheres in the presence and absence of $T_3$ 5nM. *Msi1* RNA has been shown to interact with the ZIKA RNA by mediation of the 3'UTR of the ZIKA virus and is required for ZIKA replication (Chavali et al., 2017). Msi1 is an important translational regulator in neuronal stem cells in both vertebrates and invertebrates which is enriched in neural progenitors at the ventricular and sub ventricular zones but absent from the cortical plate (Chavali et al., 2017). We had previously shown that this gene is downregulated *in vivo* in mice subventricular zone by $T_3$/TRα during progenitor to neuroblast commitment (López-Juárez et al., 2012). We analyzed the regulatory element upstream of human *MSI1* gene by NHR scan, finding that this sequence contains a number of DR4 type response elements, i.e. potential TR binding sites (Chang and

13

Pan, 1998; Paquette et al., 2014; Quack et al., 2002). A recent study compared neuroprogenitor cells (NPCs) from twins discordant for Congenital Zika Syndrome (CZS) displayed differences in NPC gene expression that could underly increased susceptibility to ZIKV-induced microcephaly through viral replication (Caires-Júnior et al., 2018).

Arguments against the implication of PPF in microcephaly have been put forward by the manufacturer, Sumitomo. In their most relevant study, Sumitomo exposed pregnant rat dams during the days 7 to 17 of gestation to dose range of PPF. The pups were then observed for physical deformations and their organs weighed. According to the producer, results did not indicate any significant changes on the nervous or reproductive systems (Saegusa, 1988). However a recent review (Parens et al., 2017) suggests that the assay may not be sufficiently sensitive and was largely restricted to analyzing impact on adult animals. Parens et al, also noticed that the report describes low brain mass and one case of microcephaly. This case was considered irrelevant by Sumitomo who argued that microcephaly should not be considered due to its dose-dependence. Parens et al., also proposed a possible mechanism of action for PPF-driven microcephaly implicating cross reactivity of PPF with retinoic acid (RA) signaling. Juvenile hormones and retinoic acid share structural similarity and it is known, that some juvenile hormones are able to bind to the retinoid acid receptor (RAR) (Harmon et al., 1995; Palli et al., 1991). They propose that PPF, a juvenile hormone analog,  binds to RAR and mimics the effect of RA, which itself has been previously connected with the induction of microcephaly (Soprano and Soprano, 1995). TH and RA interact during neurogenesis (Gil-Ibáñez et al., 2014), with RA and TR binding to nuclear receptors of steroid/thyroid hormone receptor superfamily, sharing certain gene response elements  (Glass et al., 1989) and their heterodimeric  retinoid X receptor (RXR) partner on DNA   (Kliewer et al., 1992; Zhang and Kahl, 1993).  It has been also demonstrated that RA and TH interact to regulate craniofacial development with RXR partially mediating their interaction (Bohnsack and Kahana, 2013).

Only  two studies, both using Zebrafish, have addressed the question of whether PPF could be implicated in microcephaly, each producing contradictory results (Dzieciolowska et al., 2017; Truong et al., 2016). One study (Truong et al., 2016) demonstrated  that PPF induces adverse morphological changes including craniofacial defects in zebrafish at 5.2 µM (1.66 mg/L) - EC50. In the behavioral test PPF at 6.4µM (2 mg/L) and 64µM (20mg/L) significantly reduced the

400  mobility of the zebrafish larvae compared to control animals. The authors concluded that the

401  developmental toxicity of PPF may not be limited only to insects (Truong et al., 2016).

## Conclusions

403  Taken together our results and previous findings we provide a range of evidence, that PPF and its

404  metabolite 4'-OH- PPF affect TH signaling, brain gene expression and behavior. We propose a

405  plausible mechanism of action, ie that changes in *musashi1* expression could exacerbate  ZIKA

406  virus infection.

## Acknowledgements

414

## Author Contributions

416  P.S., J.B.F and B.D. designed the study. P.S. carried out the *in vivo* experiments and analyzed the

417  data. S.L. helped with the immunohistochemistry. K.W. and T.V. carried out the *in vitro*

418  experiments. B.M. carried out the *in silico* study. M.L. helped with the fluorescence read-out,

419  immunohistochemistry, brain dissections and prepared Xenopus breedings. P.S, J.B.F., and B.D.

420  wrote the paper. All authors discussed the results and commented on the manuscript.

421

## References

de Albuquerque, M. de F.P.M., de Souza, W.V., Mendes, A. da C.G., Lyra, T.M., Ximenes, R.A., Araújo, T.V., Braga, C., Miranda-Filho, D.B., Martelli, C.M., and Rodrigues, L.C. (2016). Pyriproxyfen and the microcephaly epidemic in Brazil - an ecological approach to explore the hypothesis of their association. Mem. Inst. Oswaldo Cruz *111*, 774–776.

Alvarado, M.G., and Schwartz, D.A. (2017). Zika Virus Infection in Pregnancy, Microcephaly, and Maternal and Fetal Health: What We Think, What We Know, and What We Think We Know. Arch. Pathol. Lab. Med. *141*, 26–32.

de Araújo, T.V.B., Rodrigues, L.C., de Alencar Ximenes, R.A., de Barros Miranda-Filho, D., Montarroyos, U.R., de Melo, A.P.L., Valongueiro, S., de Albuquerque, M. de F.P.M., Souza, W.V., Braga, C., et al. (2016). Association between Zika virus infection and microcephaly in Brazil, January to May, 2016: preliminary report of a case-control study. Lancet Infect. Dis. *16*, 1356–1363.

Belenguer, V., Martinez-Capel, F., Masiá, A., and Picó, Y. (2014). Patterns of presence and concentration of pesticides in fish and waters of the Júcar River (Eastern Spain). J. Hazard. Mater. *265*, 271–279.

Bernal, J. (2005). Thyroid Hormones and Brain Development. In Vitamins & Hormones, (Academic Press), pp. 95–122.

Bohnsack, B.L., and Kahana, A. (2013). Thyroid Hormone and Retinoic Acid Interact to Regulate Zebrafish Craniofacial Neural Crest Development. Dev. Biol. *373*, 300–309.

Butler, D. (2016a). Brazil asks whether Zika acts alone to cause birth defects. Nature *535*, 475–476.

Butler, D. (2016b). Zika virus: Brazil's surge in small-headed babies questioned by report. Nature *530*, 13–14.

Caires-Júnior, L.C., Goulart, E., Melo, U.S., Araujo, B.H.S., Alvizi, L., Soares-Schanoski, A., Oliveira, D.F., Kobayashi, G.S., Griesi-Oliveira, K., Musso, C.M., et al. (2018). Discordant congenital Zika syndrome twins show differential in vitro viral susceptibility of neural progenitor cells. Nat. Commun. *9*, 475.

Chang, C., and Pan, H.J. (1998). Thyroid hormone direct repeat 4 response element is a positive regulatory element for the human TR2 orphan receptor, a member of steroid receptor superfamily. Mol. Cell. Biochem. *189*, 195–200.

Chavali, P.L., Stojic, L., Meredith, L.W., Joseph, N., Nahorski, M.S., Sanford, T.J., Sweeney, T.R., Krishna, B.A., Hosmillo, M., Firth, A.E., et al. (2017). Neurodevelopmental protein Musashi-1 interacts with the Zika genome and promotes viral replication. Science *357*, 83–88.

Dzieciolowska, S., Larroque, A.-L., Kranjec, E.-A., Drapeau, P., and Samarut, E. (2017). The larvicide pyriproxyfen blamed during the Zika virus outbreak does not cause microcephaly in zebrafish embryos. Sci. Rep. *7*, 40067.

459  Evans, D., Nijhout, F., Parens, R., Morales, A.J., and Bar-Yam, Y. (2016). A Possible Link
460  Between Pyriproxyfen and Microcephaly. BioRxiv 048538.

461  Faizan, M.I., Abdullah, M., Ali, S., Naqvi, I.H., Ahmed, A., and Parveen, S. (2016). Zika Virus-
462  Induced Microcephaly and Its Possible Molecular Mechanism. Intervirology *59*, 152–158.

463  Fini, J.B., Le Mével, S., Palmier, K., Darras, V.M., Punzon, I., Richardson, S.J., Clerget-
464  Froidevaux, M.S., and Demeneix, B.A. (2012). Thyroid hormone signaling in the Xenopus laevis
465  embryo is functional and susceptible to endocrine disruption. Endocrinology *153*, 5068–5081.

466  Fini, J.-B., Mughal, B.B., Mével, S.L., Leemans, M., Lettmann, M., Spirhanzlova, P., Affaticati,
467  P., Jenett, A., and Demeneix, B.A. (2017). Human amniotic fluid contaminants alter thyroid
468  hormone signalling and early brain development in Xenopus embryos. Sci. Rep. *7*, 43786.

469  Fujimori (1999). Toxicological evaluations (Rome).

470  Gil-Ibáñez, P., Bernal, J., and Morte, B. (2014). Thyroid Hormone Regulation of Gene
471  Expression in Primary Cerebrocortical Cells: Role of Thyroid Hormone Receptor Subtypes and
472  Interactions with Retinoic Acid and Glucocorticoids. PLOS ONE *9*, e91692.

473  Glass, C.K., Lipkin, S.M., Devary, O.V., and Rosenfeld, M.G. (1989). Positive and negative
474  regulation of gene transcription by a retinoic acid-thyroid hormone receptor heterodimer. Cell *59*,
475  697–708.

476  van Gucht, A.L.M., Meima, M.E., Zwaveling-Soonawala, N., Visser, W.E., Fliers, E., Wennink,
477  J.M.B., Henny, C., Visser, T.J., Peeters, R.P., and van Trotsenburg, A.S.P. (2016). Resistance to
478  Thyroid Hormone Alpha in an 18-Month-Old Girl: Clinical, Therapeutic, and Molecular
479  Characteristics. Thyroid Off. J. Am. Thyroid Assoc. *26*, 338–346.

480  Harmon, M.A., Boehm, M.F., Heyman, R.A., and Mangelsdorf, D.J. (1995). Activation of
481  mammalian retinoid X receptors by the insect growth regulator methoprene. Proc. Natl. Acad.
482  Sci. U. S. A. *92*, 6157–6160.

483  Invest, J.F., and Lucas, J.R. (2008). Pyriproxyfen as mosquito larvicide.

484  Kliewer, S.A., Umesono, K., Mangelsdorf, D.J., and Evans, R.M. (1992). Retinoid X receptor
485  interacts with nuclear receptors in retinoic acid, thyroid hormone and vitamin D3 signalling.
486  Nature *355*, 446–449.

487  Korevaar, T.I.M., Muetzel, R., Medici, M., Chaker, L., Jaddoe, V.W.V., Rijke, Y.B. de, Steegers,
488  E.A.P., Visser, T.J., White, T., Tiemeier, H., et al. (2016). Association of maternal thyroid
489  function during early pregnancy with offspring IQ and brain morphology in childhood: a
490  population-based prospective cohort study. Lancet Diabetes Endocrinol. *4*, 35–43.

491  Lim, W., Nguyen, N.-H., Yang, H.Y., Scanlan, T.S., and Furlow, J.D. (2002). A thyroid hormone
492  antagonist that inhibits thyroid hormone action in vivo. J. Biol. Chem. *277*, 35664–35670.

493  López-Juárez, A., Remaud, S., Hassani, Z., Jolivet, P., Pierre Simons, J., Sontag, T., Yoshikawa,
494  K., Price, J., Morvan-Dubois, G., and Demeneix, B.A. (2012). Thyroid hormone signaling acts as

495  a neurogenic switch by repressing Sox2 in the adult neural stem cell niche. Cell Stem Cell *10*,
496  531–543.

497  Morreale de Escobar, G., Obregon, M.J., and Escobar del Rey, F. (2004). Role of thyroid
498  hormone during early brain development. Eur. J. Endocrinol. *151 Suppl 3*, U25-37.

499  van Mullem, A., van Heerebeek, R., Chrysis, D., Visser, E., Medici, M., Andrikoula, M.,
500  Tsatsoulis, A., Peeters, R., and Visser, T.J. (2012). Clinical phenotype and mutant TRα1. N.
501  Engl. J. Med. *366*, 1451–1453.

502  de Oliveira, W.K., de França, G.V.A., Carmo, E.H., Duncan, B.B., de Souza Kuchenbecker, R.,
503  and Schmidt, M.I. (2017). Infection-related microcephaly after the 2015 and 2016 Zika virus
504  outbreaks in Brazil: a surveillance-based analysis. Lancet Lond. Engl. *390*, 861–870.

505  Ose, K., Miyamoto, M., Fujisawa, T., and Katagi, T. (2017). Bioconcentration and Metabolism of
506  Pyriproxyfen in Tadpoles of African Clawed Frogs, Xenopus laevis. J. Agric. Food Chem. *65*,
507  9980–9986.

508  Palli, S.R., Riddiford, L.M., and Hiruma, K. (1991). Juvenile hormone and "retinoic acid"
509  receptors in Manduca epidermis. Insect Biochem. *21*, 7–15.

510  Paquette, M.A., Atlas, E., Wade, M.G., and Yauk, C.L. (2014). Thyroid hormone response
511  element half-site organization and its effect on thyroid hormone mediated transcription. PloS One
512  *9*, e101155.

513  Parens, R., Nijhout, H.F., Morales, A., Costa, F.X., and Bar-Yam, Y. (2017). A Possible Link
514  Between Pyriproxyfen and Microcephaly. PLOS Curr. Outbreaks.

515  Pop, V.J., Kuijpens, J.L., van Baar, A.L., Verkerk, G., van Son, M.M., de Vijlder, J.J., Vulsma,
516  T., Wiersinga, W.M., Drexhage, H.A., and Vader, H.L. (1999). Low maternal free thyroxine
517  concentrations during early pregnancy are associated with impaired psychomotor development in
518  infancy. Clin. Endocrinol. (Oxf.) *50*, 149–155.

519  Quack, M., Frank, C., and Carlberg, C. (2002). Differential nuclear receptor signalling from
520  DR4-type response elements. J. Cell. Biochem. *86*, 601–612.

521  REDUAS (2016). REPORT from Physicians in the Crop-Sprayed Town regarding Dengue-Zika,
522  microcephaly, and massive spraying with chemical poisons.

523  Rodrigues, L.C., and Paixao, E.S. (2017). Risk of Zika-related microcephaly: stable or variable?
524  Lancet Lond. Engl. *390*, 824–826.

525  Saegusa, T. (1988). Study of S-31183 by oral administration during the period of fetal
526  organogenesis in rats (Osaka, Japan: Sumitomo Chemical Co.).

527  Soprano, D.R., and Soprano, K.J. (1995). Retinoids as teratogens. Annu. Rev. Nutr. *15*, 111–132.

528  Truong, L., Gonnerman, G., Simonich, M.T., and Tanguay, R.L. (2016). Assessment of the
529  developmental and neurotoxicity of the mosquito control larvicide, pyriproxyfen, using
530  embryonic zebrafish. Environ. Pollut. Barking Essex 1987 *218*, 1089–1093.

531    US EPA (2011). Pyriproxyfen.

532    Wegner, S., Browne, P., and Dix, D. (2016). Identifying reference chemicals for thyroid
533    bioactivity screening. Reprod. Toxicol. Elmsford N *65*, 402–413.

534    WHO (2007). Pyriproxyfen  in  drinking-water:  Background  document  for  development
535    of  WHO  guidelines  for    drinking-water quality. World Health Organ.
536    WHOSDEWSH070110.

537    Wilson, T.G. (2004). The molecular site of action of juvenile hormone and juvenile hormone
538    insecticides during metamorphosis: how these compounds kill insects. J. Insect Physiol. *50*, 111–
539    121.

540    Yoshino, H., Kaneko, H., Nakatsuka, I., and Yamada, H. (1995). Metabolism of Pyriproxyfen. 2.
541    Comparison of in Vivo Metabolism between Rats and Mice. J. Agric. Food Chem. *43*, 2681–
542    2686.

543    Zhang, X.K., and Kahl, M. (1993). Regulation of retinoid and thyroid hormone action through
544    homodimeric and heterodimeric receptors. Trends Endocrinol. Metab. TEM *4*, 156–162.

545    Zhang, L., Harada, K., and Shono, T. (1998). Cross resistance to insect growth regulators in
546    pyriproxyfen-resistant housefly. Appl. Entomol. Zool. *33*, 195–197.
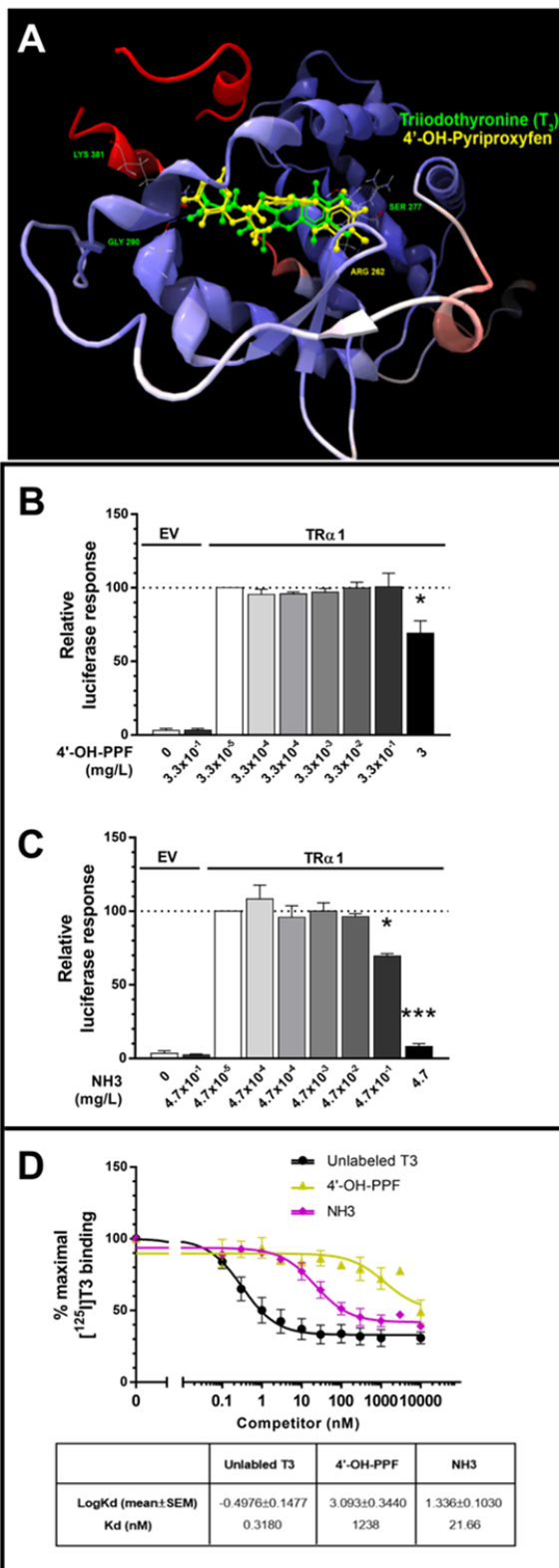
547

548

549    **Graphical abstract**
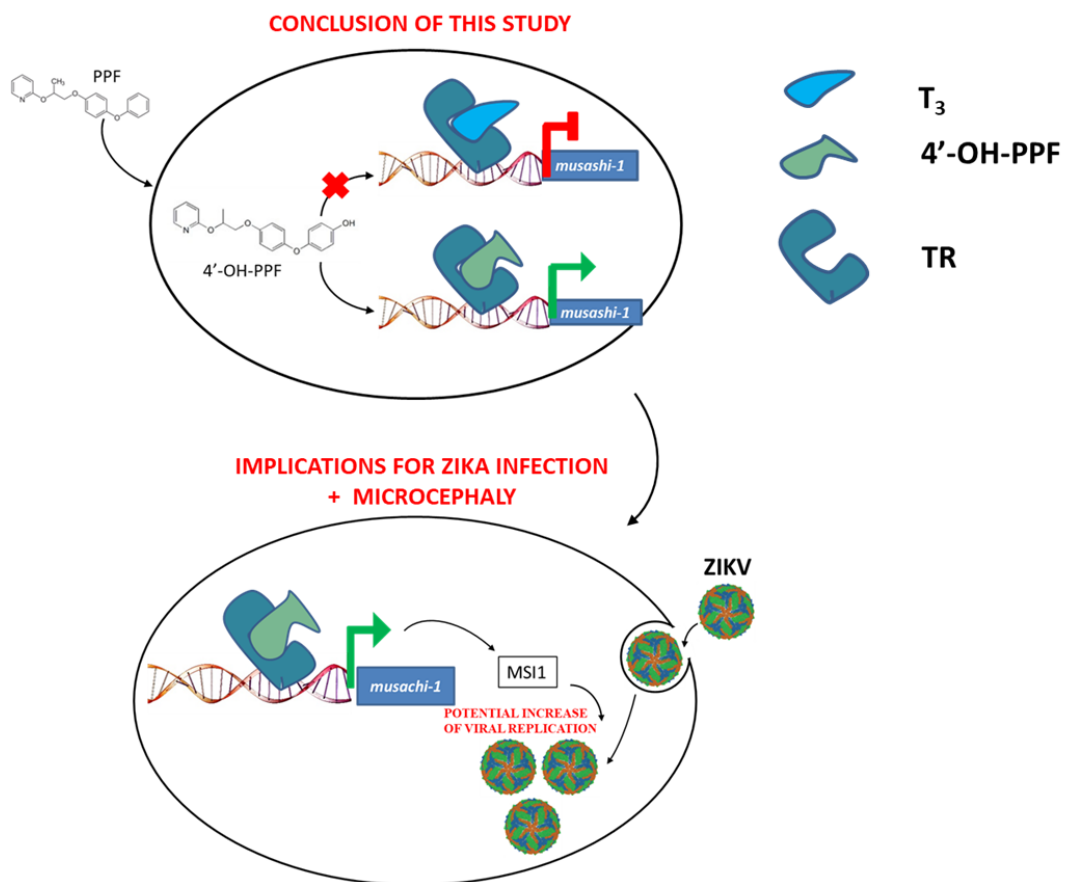


550

551

552 **Figures**

555 **Figure 1. 4'-OH-PPF acts as Thrα antagonist with affinity 50x lower than NH3.** (**A**) Docking

556 result of Triiodothyronine (T3) and 4'-OH-Pyriproxifen on the crystal structure of human thyroid

557 hormone receptor alpha (TRα, 4LNW). <10,000 iterations were run for each ligand within the $T_3$

558 binding pocket, with top 10 docking results analysed for varying conformations using CLC Drug

559 Discovery 3. Ligand docking of triiodothyronine ($T_3$) with three hydrogen bonds are; $LYS^{381}$,

560 $GLY^{290}$ and $SER^{277}$ for TRα. Ligand docking of 4'OH-Pyriproxyfen with one hydrogen bond is

561 $ARG^{262}$ for TRα. $T_3$ and 4'-OH-Pyriproxifen ligands show comparative binding scores -65.25

562 and -77.33 respectively for TRα. These scores predict a strong steric fit of 4'-OH-Pyriproxifen

563 into the $T_3$ binding pocket. (**B-C**) The transcriptional activity of TRα1 stimulated by 1 nM T3

564 was significantly reduced by increasing concentrations of 4'-OH-PPF (**B**) and NH3 (**C**) (EV:

565 empty vector control). The data are presented as mean±SEM of two independent experiments

566 performed in triplicate (One-way ANOVA $p<0.05$; Tukey's post-test compared to 0 nM

567 competitor, $*p<0.05$, $**p<0.01$, $***p<0.001$).   (**D**) $[^{125}I]T3$ dissociation curves showing the

568 affinity of TRα1 for 4'-OH-PPF and NH3. High concentrations of 4'-OH-PPF and NH3 reduced

569 TR-bound $[^{125}I]T3$, indicating competitive binding to TRα1. 10000 nM of 4'-OH-PPF and NH3

570 corresponds to 3 mg/L and 4.7 mg/L respectively. The affinity of TRα1 for 4'-OH-PPF was

571 lower than for NH3, indicated by the right-shift of the curve and higher Kd for 4'-OH-PPF. The

572 data are presented as mean±SEM of at least two independent experiments performed in duplicate.

573
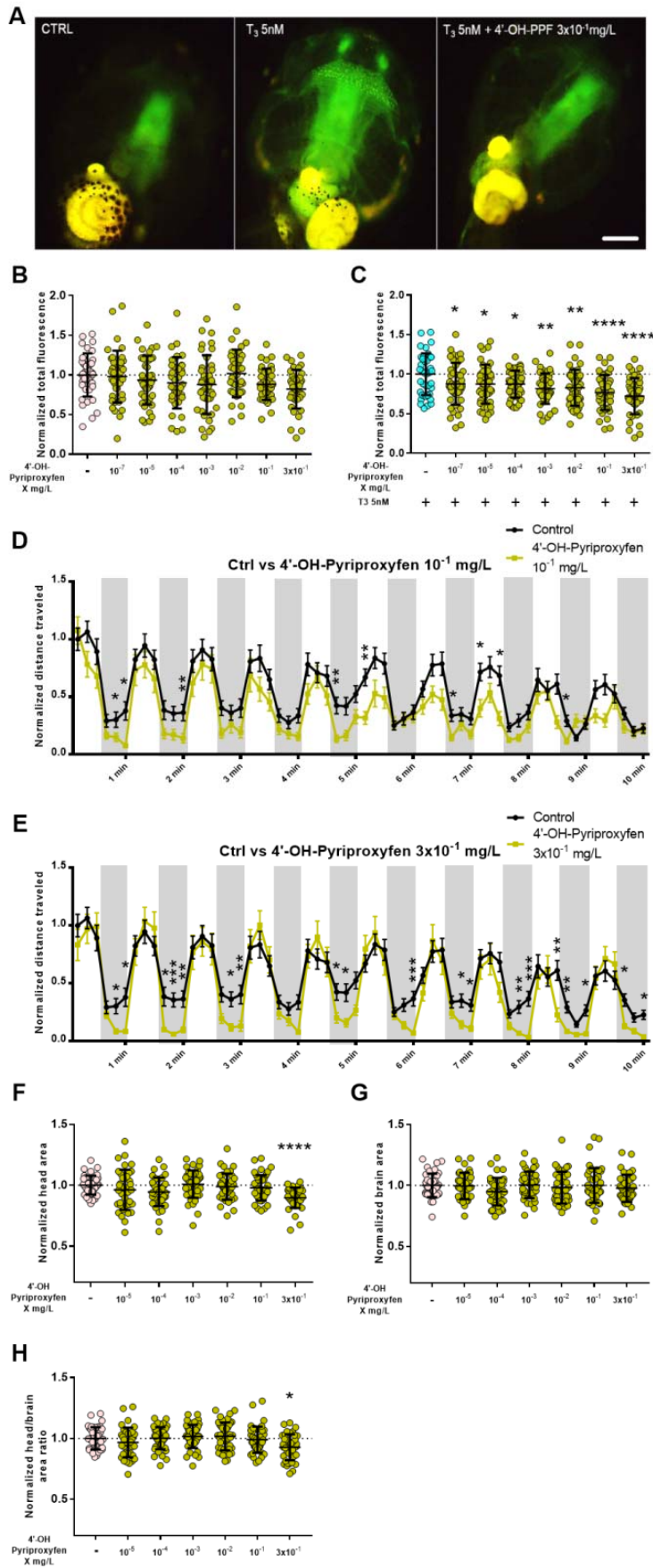
**Figure 2. 4'-OH-PPF affects thyroid hormon signalling and mobility of *Xenopus laevis* tadpoles. (A)** Tg(*thibz*:GFP) tadpoles exposued for 72h to (from left to right) vehicle control, $T_3$ 5nM and $T_3$ 5nM+ 4'-OH-PPF $3x10^{-1}$mg/L. Scale bar 500 μm. **(B-C)** 72 hours exposure of st 45 Tg(*thibz*:GFP) *Xenopus laevis* tadpoles to 4'-OH- PPF in the absence **(B)** or presence of $T_3$ 5nM **(C)**. Values normalized to control group **(B)** or $T_3$ group **(C)**. Pool of 3 independent experiments; n=15 per experiment. One-way ANOVA with Dunn's post test (Mean ± SDs, *P < 0.05, **P < 0.01, ***P < 0.001, ****P < 0.001). **(D-E)** Total distance travelled by tadpoles exposed to 4'-OH-PPF. 10 minute trial, distance traveled counted every 10 seconds. Dark background represents dark period, white background represents light period. Values normalized to first 10 second period of control group. Pool of 3 independent experiments; n= 12 per experiment. Kruskal-Wallis (Mean ± SEM, *P<0.05, **P < 0.01, ***P < 0.001). **(F-H)** Area of the head **(F)**, brain **(G)** and head/brain ration **(H)** of st45 *Xenopus laevis* tadpole exposed to 4'-OH-PPF during 72h. Values normalized to control group. Pool of 3 independent experiments; n=15 per experiment. One-way ANOVA with Dunn's post test (Mean ± SDs, *P<0.05, ****P < 0.001).

589

590

591

592
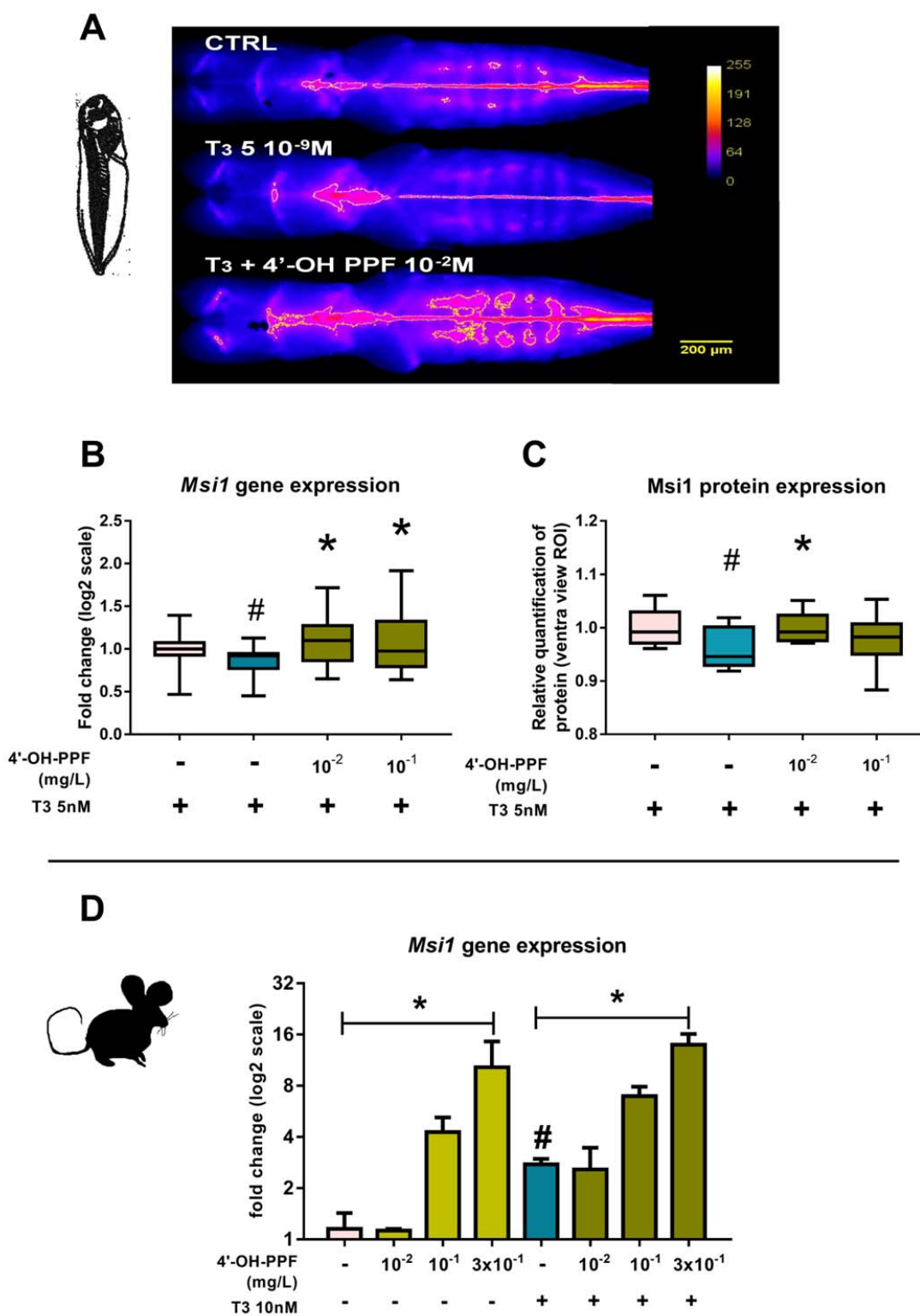
**Figure 3 :** *Musashi1* **gene expression and expression of its encoded protein is modified by TH and 4-OH-PPF.** (**A**) Representative pictures of immunohistochemistry realized on solvent control, $T_3$ 5nM and $T_3$+ 4'-OH-PPF $10^{-2}$ mg/L, ROI is delimited by thin white line. (**B**) *Msi1* gene expression on dissected brains from NF46 tadpoles exposed for 24h to 4'-OH-PPF ($10^{-2}$; $10^{-1}$ mg/L) in challenge with $T_3$ 5nM. (**C**) Msi1 protein expression on dissected brains from NF46 tadpoles exposed for 24h to 4'-OH-PPF ($10^{-2}$; $10^{-1}$ mg/L) in challenge with $T_3$ 5nM. Antibody Alexa Fluor 488-conjugated anti-rabbit. Quantification of the protein level based on fluorescence intensity from dorsal views. Two independent experiments in case of protein expression study with 4 to 10 tadpoles per experiment were done. Three independent experiments in the case of gene expression study, n=5 per experiment. (**D**) *Msi1* gene expression in mouse neurospheres after 7 days of proliferation. Graphs represent the pool of the experiments (each normalized to its own control). Non-parametric ANOVA ; Kruskal-Wallis with Dunnet's post test. *$p<0.05$. Statistics comparing $T_3$ with control - Mann-Whitney; # $p<0.05$.

606